Electric current and phase-boundary potential for electrode reaction in phase-field model

Yoshinao Okajima, Yasushi Shibuta, Toshio Suzuki

Department of Materials Engineering, Graduate School of Engineering, The University of Tokyo.

7-3-1 Hongo, Bunkyo-ku, Tokyo 113-8656, Japan

E-mail: okajima@mse.mm.t.u-tokyo.ac.jp

1. Introduction

A phase-field model (PFM) for electrochemistry, in which cations are driven by external charge with thermodynamics potential, has been reported about a bridge formation process in nanometer-scale switch and an electrodeposition process. However, a phase-boundary potential could not be expressed explicitly since the difference of inner potential between two phases was ignored in these models. In this study, the PFM, which can treat the electrical current across the interface and phase-boundary potential, is formulated on the basis of the concepts of our previous model and the Poisson-Nernst-Planck (PNP) equation[3].

Contents:
- Phase-boundary potential in 1-D and 2-D equilibrium states.
- Growth analysis in 1-D steady state.
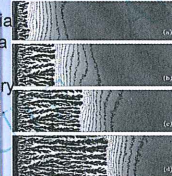- Stability and instability analysis in 2-D.

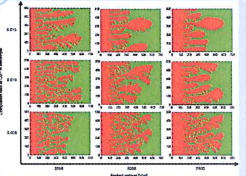Fig. 1-1 Dense growth from cupric acetate solution in thin cell[1].

Fig. 1-2 Morphological diagram for copper electrodeposition [2].

2. Methodology

PFM for electrochemistry

Free energy density of system and boundary condition at interface:

$$f_V(\xi,C_M,C_A)=f^\alpha p(\xi)+\left[f^\beta+C_M^\beta\Delta\mu_M\right](1-p(\xi))+Wg(\xi)$$

$$\frac{df^\alpha}{dC_M^\alpha}=\frac{df^\beta}{dC_M^\beta}+\Delta\mu_M$$

f_V; free energy density, α, β; electrode, electrolyte phase
ξ; phase-field, C; concentration
$\Delta\mu_M$; chemical potential difference, W; double-well potential

PF equation:

$$\frac{\partial\xi}{\partial t}=M_\xi\left[\kappa_\xi^2\nabla^2\xi+\frac{\partial p(\xi)}{\partial\xi}\frac{1}{\overline{V}_m}\left(RT\ln\frac{C_M^\alpha\,{}^eC_M^\beta}{C_M^\beta\,{}^eC_M^\alpha}+(z_M+1)\Delta\mu_{M^{z+}}\right)-W\frac{dg(\xi)}{d\xi}\right]$$
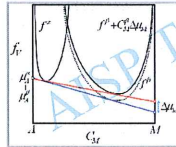
Diffusion equation:

$$\frac{\partial C_M}{\partial t}=\nabla\left[D_{M^+}\left\{P(\xi)C_M^\alpha(1-C_M^\alpha)+(1-P(\xi))C_M^\beta(1-C_M^\beta)\right\}\nabla\left(\ln\frac{C_M^\beta}{1-C_M^\beta}+\frac{z_M F\psi}{RT}\right)\right]$$

Conservation of charge equation:

$$\nabla\cdot\vec{i}(\xi,\phi)=0 \qquad (\phi=\psi+\chi)$$

R; gas constant, T; temperature, F; Faraday constant, z; valence, M_ξ; PF mobility, κ_ξ; coefficient of energy gradient, ${}^eC$; equilibrium concentration, V_m; molar volume

Electrical current at the electrode-electrolyte interface

$$\vec{i}(\xi,\phi)=-\sum_j\frac{\sigma_j(\xi)}{Fz_j}\nabla\left[\overline{\mu}_j^\alpha(C_j^\alpha,\phi)p(\xi)+\overline{\mu}_j^\beta(C_j^\beta,\phi)(1-p(\xi))\right]$$

phase-fraction function : $p(\xi)=\xi^3(6\xi^2-15\xi+10)$

M⁺	M⁺
	A
$\xi=1$	$\xi=0$
Electrode:α	Electrolyte: β

The electrical current is rewritten by assumption that the electrical conductors of electrode and electrolyte are cation of M^{z+}:

$$\vec{i}_{M^{z+}/M^{z+}}(\xi,\phi)=-\frac{\sigma_{M^{z+}}(\xi)}{Fz_M}\nabla\left[\frac{1}{z_M+1}\left\{RT\ln C_{M^{z+}}^\alpha-\left(RT\ln\frac{{}^eC_{M^{z+}}^\alpha}{{}^eC_{M^{z+}}^\beta}\frac{C_{M^{z+}}^\beta}{C_{M^{z+}}^\alpha}\right)\right\}p(\xi)+Fz_M\phi\right]$$

Nernst equation can be derived from $\vec{i}_{M^{z+}/M^{z+}}(\xi,\phi)=0$.

Simulation methodology

For separating external potential and surface potential from electric potential, the external potential connects smoothly at the interface of the electrode and electrolyte, when the point of the phase 0.2 is defined as the boundary of the surface potential.

parameters			
Diffusion coefficient	α	$D_{M^+}^\alpha$ / m^2s^{-1}	3.7×10^{-13}
	β	$D_{M^+}^\beta$ / m^2s^{-1}	3.7×10^{-10}
Electrical conductivity	α	$\sigma_{M^+}^\alpha$ / $m^{-1}\Omega^{-1}$	5.9×10^2
	β	$\sigma_{M^+}^\beta$ / $m^{-1}\Omega^{-1}$	2.7
Partial molar volume		$\overline{V}_m$ / m^3mol^{-1}	1.0×10^{-5}
Interfacial energy		γ / Jm^{-2}	9.3

3. Result and Discussion
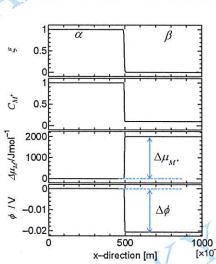
Phase-boundary potential in equilibrium state

Fig. 3-1 Distributions of ξ, C_{M+}, $\Delta\mu_{M+}$ and ϕ in equilibrium state.

The equilibrium distributions is shown in the left half of the system, when $\Delta\mu_{M+}$=2000 Jmol⁻¹ in the system with the monovalence (z = 1) component.

Nernst relation

In 1-D equilibrium state, the chemical potential difference and the phase-boundary potential satisfied the relation of Nernst equation in every valence.
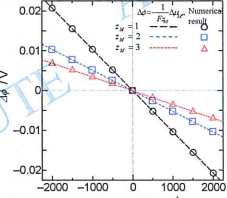

Fig. 3-2 Relation of the electrode potential with Nernst equation.

Gibbs-Thomson effect

The following equation is derived from Nernst equation and Gibbs-Thomson equation:

$$\Delta\phi(\infty)-\Delta\phi(r)=\frac{1}{Fz_M}\frac{\overline{V}_m}{(z_M+1)}\gamma\frac{1}{r}$$
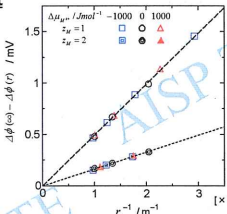
The numerical results agreed with this equation.

Fig. 3-3 Gibbs-Thomson effect of the electrode/electrolyte interface.

Steady growth of the electrode in 1-D

The dependence of the growth velocity of electrodeposits on the applied voltage and phase-boundary potential was examined using a 1-D system.

$$v\cong\frac{1}{{}^eC_M^\alpha-{}^eC_M^\beta}J_M^\beta$$

$$\cong\frac{1}{{}^eC_M^\alpha-{}^eC_M^\beta}D_M^\beta\frac{Fz_M}{RT}{}^eC_M^\beta\exp\left\{-\frac{Fz_M(z_M+1)}{RT}\Delta\phi\right\}$$

$$\times\left[1-{}^eC_M^\beta\exp\left\{-\frac{Fz_M(z_M+1)}{RT}\Delta\phi\right\}\right]\Delta V$$

This equation, which is derived from the diffusion eq., the PF eq. and Nernst eq., indicates dashed lines in these figures.

The growth velocity had a positive correlation with the applied voltage and a negative correlation with the phase-boundary potential.
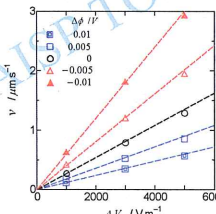

Fig. 3-4 Interface velocity as a function of the applied voltage.

Fig. 3-5 Interface velocity as a function of the phase-boundary potential.

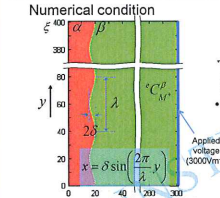### Stability analysis of the electrode-electrolyte interface in 2-D

Fig. 3-6 Initial distribution of ξ in 2-dimensional system. The γ was set to be 0.93.
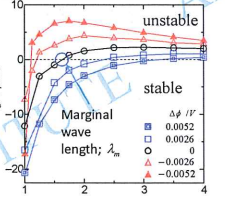

Fig. 3-7 Development of perturbation at electrode/electrolyte interface.
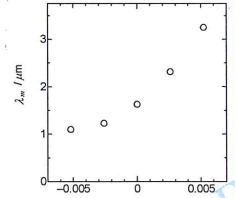

Fig. 3-8 Marginal wave length as a function of the phase-boundary potential.

The stable and unstable condition of interface was obtained from a time variation of amplitude, $\dot\delta$, as a function of wavelength (Fig. 3-7). The obtained marginal wavelength had a positive correlation with the phase-boundary potential(Fig. 3-8). In addition, the marginal wavelength has proportional relationship with tip radius, ρ, in steady growth(Fig. 3-10).
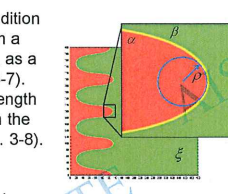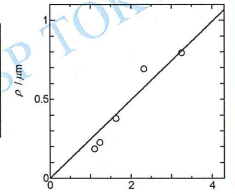

Fig. 3-9 Tip radius in stability growth.

Fig. 3-10 Relation of curvature radius with marginal wave length.

Instability growth in 2-D

conditions
$C_0=0.015$
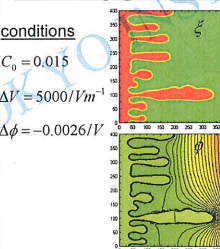$\Delta V=5000/Vm^{-1}$
$\Delta\phi=-0.0026/V$

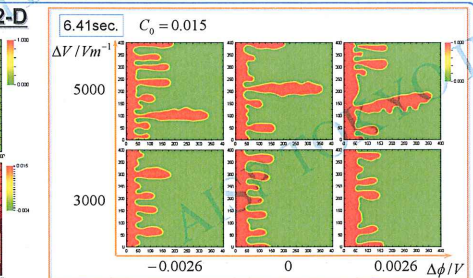Fig. 3-11 Snapshots of distributions of ξ and ϕ in 2-dimensional system.

Fig. 3-12 Morphological diagram as functions of applied voltage and phase-boundary potential.

Tips of α-phase developed to direction of x, since the gradient of the electric potential was concentrated in top of the tips (Fig. 3-11). The morphology that disturbed the interface appeared conspicuously as the phase-boundary potential was negative(Fig. 3-12).

4. Conclusion

In this study, a phase-field model (PFM), which can treat the electrical current across the interface and phase-boundary potential, was newly formulated to analyze an electrode-electrolyte reaction. Using this model, it was confirmed that the relation between the chemical potential difference and the phase-boundary potential satisfied the Nernst and the Gibbs-Thomson. Related to the kinetics of the electrode-electrolyte interface, the dependence of the growth velocity of electrodeposits on the applied voltage and the stability of the electrode-electrolyte interface during electrodeposition were examined as a function of the phase-boundary potential.

[1]. C. Leger et al., Phys. Rev. E, 61 (2000) 5452. [2] Y. Shibuta et al., Sci. Tecnol. Adv. Mater., 8 (2007) 511. [3] Z. Shuss et al., Phys. Rev. E, 64 (2001) 036116.